CrossMark

Boundary layer perspective assessment of air pollution status in Wuhan city from 2013 to 2017

Yassin Mbululo (ORCID) **· Jun Qin · Zhengxuan Yuan ·**
Fatuma Nyihirani · Xiang Zheng

Abstract This study used daily air pollution data
($PM_{2.5}$, PM_{10}, SO_2, NO_2, CO, and O_3) from nine mon-
itoring stations in Wuhan city to calculate the air quality
index (AQI) from 2013 to 2017. Together with this data,
L-band sounding data, ground meteorological data, and
air mass back trajectories were also used to describe the
dynamics of atmospheric boundary layer (ABL) during
pollution process. Analysis of the results shows that,
even though the city is still polluted, the number of
polluted days was decreasing. Ranking the years in
terms of pollution status shows that the year 2013 was
the most polluted year while the year 2017 was the
cleanest year. Average annual limit of PM_{10}, $PM_{2.5}$,
and NO_2 during these 5 years were 1.3~1.8, 1.5~2.7,
and 1.2~1.5 times higher than the annual average ac-
ceptable limit, respectively. The average ratio of $PM_{2.5}$/
PM_{10} for 5 years was 0.67 which signifies that a
significant portion of $PM_{2.5}$ accounted for the total mass
of PM_{10}. Moreover, the condition of ABL during the
pollution process shows the dominance of strong
ground inversion and weak to calm winds. These con-
ditions are not favorable for horizontal and vertical
mixing of air pollutants and prevent dilution of pollut-
ants with clean air. Mean cluster analysis of air mass
back trajectory shows that pollutants of local origin were
more important than the trans-boundary movement of
air pollutants. This indicates that the observed pollution
in Wuhan was more of local origin.

Y. Mbululo · J. Qin (✉) · Z. Yuan · F. Nyihirani · X. Zheng
School of Environmental Studies, China University of
Geosciences, 388 Lu Mo Road, Wuhan 430074, China
e-mail: qinjun@cug.edu.cn

Y. Mbululo
Department of Geography and Environmental Studies, Solomon
Mahlangu College of Science and Education, Sokoine University
of Agriculture, Morogoro, Tanzania

F. Nyihirani
Centre for Environment, Poverty and Sustainable Development,
Mzumbe University, Morogoro, Tanzania

Introduction

Air pollution in China has become an issue of concern
not only within the Chinese community but also to the
neighboring countries. This is because, the pollutants
which originate in industrialized regions in China have
been observed to affect other countries as a result of
trans-boundary movement (Inomata et al. 2009; Jeong
et al. 2011; Lee et al. 2013; Lu et al. 2016). China which
is the fastest growing economy at the pace which has
never been seen before is facing a serious air pollution
problem (Feng et al. 2015; Li et al. 2017; Liu et al. 2013;
Ran et al. 2009). Moreover, the air pollution problem
seems to be universal as the report by World Health
Organization (WHO) indicates that people living in
cities are no longer safe, as 90% of the people live in

🖄 Springer

cities which do not comply with the WHO air quality guideline (AQG) (WHO 2016). The report went further by revealing the sore fact that 10% of the annual deaths happen as a result of air pollution, while outdoor pollution on its own is responsible for the killing of around three million people each year. In an effort to combat the air pollution problems, the Chinese Ministry of Environmental Protection (CMEP) ratified National Ambient Air Quality Standard (NAAQS) in 2012. This new guideline aims at regulating the emission of six principal pollutants (i.e., NO_2, SO_2, CO, O_3, $PM_{2.5}$, and PM_{10}) which are used to calculate the Air Quality Index (AQI) for cities. The set limit for daily (24 h average) concentration of PM_{10}, $PM_{2.5}$, SO_2, NO_2, CO, and 8 h average concentration of ozone are 150 $\mu g/m^3$, 75 $\mu g/m^3$, 150 $\mu g/m^3$, 80 $\mu g/m^3$, 4 mg/m^3, and 160 $\mu g/m^3$, respectively (GB3095 2012). It is worth to note that the standard set in NAAQS are 1.6~7.5 times higher than the standard which have been suggested by WHO for daily PM_{10}, $PM_{2.5}$, SO_2, NO_2, and 8 h average ozone of 50 $\mu g/m^3$, 25 $\mu g/m^3$, 20 $\mu g/m^3$, 40 $\mu g/m^3$, and 100 $\mu g/m^3$, respectively.

Wuhan (29°58′~31°22′ N and 113°41′~115°05′ N), the capital city of Hubei province, is one of the megacities in central China. This city which is the hub of transportation and the major link of west and east China is reported to be polluted by a number of studies. For instance, Lyu et al. (2016) advocate Wuhan as one of the polluted cities because during their study period, they observed PM_{10} and $PM_{2.5}$ frequently exceeding the NAAQS as a result of intensive biomass burning. The authors documented the average concentration of $PM_{2.5}$ of 81.2 $\mu g/m^3$ in summer and 85.3 $\mu g/m^3$ in autumn. Wang et al. (2016) revealed the exceedance of annual average concentration of $PM_{2.5}$, PM_{10}, and NO_2 stipulated in NAAQS by 256%, 192%, and 137%, respectively. Notably, monthly average concentration of $PM_{2.5}$ was highest in December (winter month) and lowest in July (summer month) as a result of precipitation. Xu et al. (2017) reported the 3 years average ratio of $PM_{2.5}$/PM_{10} of 0.62, the ratio which is higher than those found in most of the Chinese cities and town. The authors further revealed the existence of gradual increase of $PM_{2.5}$/PM_{10} ratio at night time and they related this increase to stable atmospheric conditions which constrained vertical airflow. Based on the NAAQS, the concentration of $PM_{2.5}$ and PM_{10} during the study period was above the daily acceptable limit by 40% and 27%, respectively. A follow-up study by Mbululo et al.

(2017) reported that 83.05% of the days in 2015 were having $PM_{2.5}$/PM_{10} ratio of more than 0.5, indicating the severity of $PM_{2.5}$ in Wuhan atmosphere. The minimum and maximum ratio of organic carbon (OC)/elementary carbon (EC) were 3.5 and 24.2, respectively, indicating that the large portion of $PM_{2.5}$ was composed of OC. A sampling campaign in spring of 2014 by Acciai et al. (2017) found average concentration of $PM_{2.5}$ to be 95.53 $\mu g/m^3$, which is higher than the acceptable limit set in NAAQS. Likewise, by using the Positive Matrix Factorization (PMF) model, the authors identified biomass burning as the largest (62.3%) contributor of $PM_{2.5}$ in Wuhan, followed by metallurgical and steel industries (14%), crustal dust (12.5%), and dust and vehicle emission (10.4%).

Based on the available literature on air quality in Wuhan, the dynamics of atmospheric boundary layer (ABL) which is the main determinant of air quality (Hu et al. 2014; Wu et al. 2013) seems to have attracted limited attention to most of the researchers. Elsewhere, a study by Li et al. (2018) analyzed the characteristics of pollutants and the boundary layer structure by using meteorological instruments which were fixed at different heights (i.e., 10, 30, 50, 70, and 100 m) on a 100-m high tower. Nevertheless, the meteorological parameters (wind speed, air temperature, and relative humidity) captured at these altitudes cannot fully describe the dynamics of the ABL accurately. This is because the average height of ABL is far higher than this altitude. A number of studies (Tang et al. 2017; Wang et al. 2017) show the need for more detailed vertical study of meteorological parameters to fully understand the dynamics of ABL. This study therefore aims at describing the vertical structure of meteorological parameters (temperature, relative humidity, wind speed, and direction) at ABL of Wuhan city during pollution process by using 5 years data spanning from 2013 to 2017. Together with these high altitudes sounding data of ABL, this study also used daily ground observation data from meteorological station, air quality data, and air mass back trajectories.

Methodology

Data and sampling sites

Average daily air pollutant data ($PM_{2.5}$, PM_{10}, SO_2, NO_2, CO, and O_3) from 2013 to 2017 from nine

monitoring stations which are distributed all over Wuhan city were used in this study. These nine stations are administered by the Chinese Ministry of Environmental Protection (CMEP) and are used to determine the AQI of the city. Together with this, daily L-band radar data at 0700 LST with a vertical resolution of 10 m was also used to describe the vertical profile of different meteorological parameters (temperature, relative humidity, wind speed, and direction) up to 3000 m. The air quality data were obtained from Wuhan Environmental Protection Agency (WHEPA), while the L-band sounding data was obtained from Wuhan Meteorological Bureau (WMB). Daily average data of $PM_{2.5}$ and AQI were used to plot the line graphs from which highly polluted and clean days could be defined. L-band sounding data were used to plot the vertical profile of the meteorological parameters.

Air quality index (AQI)

The overall AQI of the city is determined by the sub-AQI of the six air pollutants (PM_{10}, $PM_{2.5}$, SO_2, NO_2, CO, and O_3) which are calculated by Eq. (1), as given in Technical Regulation on Ambient Air Quality Index (HJ633-2012, 2012). The overall AQI represents the maximum of the sub-AQI of all pollutants according to Eq. (2). Higher values of AQI are associated with "bad" while lower values are associated with "good" condition of air.

$$IAQI_p = \frac{I_{high} - I_{low}}{C_{high} - C_{low}} \left(C_p - C_{low} \right) + I_{low} \qquad (1)$$

$$AQI = \max(I_1, I_2, \ldots, I_n) \qquad (2)$$

where $IAQI_p$ is the air quality sub index for air pollutant p, C_p is the concentration of pollutant p, C_{low} is the concentration breakpoint that is $\leq C_p$, C_{high} is the concentration breakpoint that is $\geq C_p$, I_{low} is the index breakpoint corresponding to C_{low}, and I_{high} is the index breakpoint corresponding to C_{high}. The daily AQIs were calculated by the 24-h average concentration of five air pollutants (PM_{10}, $PM_{2.5}$, SO_2, NO_2, and CO) and the daily average 8 h maximum concentration of O_3. Table 1 summarizes the China air quality grading standard while the reference concentrations and index of pollutants can be found in HJ633-2012 2012.

Table 1 China air quality grading standards

Air quality index (AQI)	Air quality index level	Air quality index category
0~50	Level 1	Excellent
51~100	Level 2	Good
101~150	Level 3	Slightly polluted
151~200	Level 4	Moderate polluted
201~300	Level 5	Heavy pollution
> 300	Level 6	Severe pollution

Air mass residence time

The movement of air parcel from one place to another acts as a transport agent of airborne particulate matter (PM). A study by Dimitriou (2015) considered the air mass residence time over specific source area to be linearly related to that area's contribution to the receptor site. This study used 72-h air mass back trajectories approaching Wuhan at 100 m, 300 m, and 500 m to calculate and analyze airflow and diffusion by using Hybrid Single-Particle Lagrangian Integrated Trajectory (HYSPLIT) model developed by the National Oceanic and Atmospheric Administration (NOAA) Air Resources Laboratory's (ARL) of the USA. This model has a relatively complete transport, diffusion, and sedimentation model for handling a variety of meteorological element input fields, multiple physical processes, and different types of pollutant emission sources (Rolph et al. 2017; Stein et al. 2015). The TrajStat software which was developed based on Geographical Information System (GIS) by Wang et al. (2009) was used to cluster air mass back trajectories using Euclidean distance. The meteorological data input for running the software were from NCEP (National Centers for Environmental Prediction) fields obtained from NOAA which were available at every 3 h with 1°×1° spatial resolution.

Potential source contribution function (PSCF)

This study also used a PSCF method to identify the major contributing sources of $PM_{2.5}$ in Wuhan city. The basis of PSCF method is that, if a receptor site is located at particular latitude and longitude, an air parcel back trajectory passing through that location indicates that the material from other sources can be transported through the trajectory to the receptor site (Dimitriou and Kassomenos 2014; Jeong et al. 2011; Polissar et al.

1999; Wang et al. 2009; Zeng and Hopke 1989). The formula, Eq. (3), defined the PSCF

$$PSCF_{(iJ)} = \frac{m_{(ij)}}{n_{(ij)}} \qquad (3)$$

where $n_{(ij)}$ is the number of times that the trajectories passed through the cell (i, j) and $m_{(ij)}$ is the number of times that the pollutant concentrations were higher at the receptor site than the set criterion. In this study, the average daily acceptable limit of $PM_{2.5}$ (75 $\mu g/m^3$) stipulated in NAAQS was set as a criterion and utilized in PSCF calculation to identify the potential source areas (PSA) at distance which are more likely to have larger impact than the local sources. To reduce uncertainties resulted from the effect of simulation results of those grids with value of $n_{(ij)}$ that are too small, an empirical weighting coefficient, $W_{(ij)}$ (Eq. (4)) was multiplied by PSCF (Dimitriou and Kassomenos 2014; Jeong et al. 2011; Polissar et al. 1999; Wang et al. 2009). For the case of this study, n_{avg} is the average value ($n_{(ij)} > 0$) of the number of all trajectory terminal points in grids.

$$W_{(i,j)} = \begin{cases} 1.0 & (3n_{avg} < n_{(i,j)}) \\ 0.7 & (1.5n_{avg} < n_{(i,j)} < 3n_{avg}) \\ 0.4 & (n_{avg} < n_{(i,j)} < 1.5n_{avg}) \\ 0.2 & n_{(i,j)} < n_{avg} \end{cases} \qquad (4)$$

Results and discussion

Analysis of pollution status

The results of six air pollutants ($PM_{2.5}$, PM_{10}, SO_2, NO_2, CO, and O_3) from nine air monitoring stations for 5 years (2013~2017) in Wuhan show that they are above the daily and annual acceptable limits set by NAAQS except for SO_2 and CO. Particulate matter ($PM_{2.5}$ and PM_{10}) pollution was serious during these 5 years. The ranking of years in the order of pollution status shows that 2013 was seriously polluted as 48% of its days were far above the $PM_{2.5}$ daily average acceptable limit of 75 $\mu g/m^3$, followed by 2014 (44%), 2015 (33%), 2016 (25%), and 2017 (20%). The same order is observed for PM_{10} as daily average acceptable limit of 150 $\mu g/m^3$ in the year 2013 was exceeded by 30%, followed by 2014 (24%), 2015 (20%), 2016 (13%), and 2017 (8%). Table 2 shows the minimum and maximum concentration of $PM_{2.5}$ and their standard

deviation. Higher concentration is dominant in winter (December to February) and lower concentration in summer (June to August) months. Looking at the annual average acceptable limit, the concentration of PM_{10}, $PM_{2.5}$, and NO_2 was also higher above the annual acceptable limit of 70 $\mu g/m^3$, 35 $\mu g/m^3$, and 40 $\mu g/m^3$ respectively. The annual limit of $PM_{2.5}$ in 2013 was 2.7 times higher than the average annual acceptable limit while for the other years, 2014, 2015, 2016, and 2017 were 2.3, 2, 1.6, and 1.5 times higher than the annual acceptable limit, respectively. For the case of PM_{10}, it was above the annual average acceptable limit in 2013, 2014, 2015, 2016, and 2017 by 1.8, 1.7, 1.5, 1.3, and 1.3 times higher than the annual acceptable limit, respectively. The annual average concentration of NO_2 was higher in 2013 by 1.5 times, 2014 by 1.3 times, and in 2015, 2016, and 2017 by 1.2 times the annual average acceptable limit. Corroborated results to this is reported by Wang et al. (2016) as they found the exceedance of annual average concentration of $PM_{2.5}$, PM_{10}, and NO_2 of 2.6, 1.9, and 1.4 times higher than the NAAQS from March 2013 to February 2014, respectively.

Moreover, the ratio of $PM_{2.5}/PM_{10}$ in 2013, 2014, 2015, 2016, and 2017 were 0.75, 0.71, 0.64, 0.63, and 0.61, respectively, indicating the significant contribution of $PM_{2.5}$ to the total mass of PM_{10}. In addition to this, the percentage of days having the $PM_{2.5}/PM_{10}$ ratio of above 0.5 in 2013, 2014, 2015, 2016, and 2017 were 83%, 89%, 78%, 69%, and 64%, respectively. Corroborated results to this have been reported in a study by Xu et al. (2017), as they reported $PM_{2.5}/PM_{10}$ ratio of 0.62 and Mbululo et al. (2017) who found percentage of days with $PM_{2.5}/PM_{10}$ ratio of above 0.5 of 83.05%. It is worth noting that $PM_{2.5}$ which is the dominant pollutant in Wuhan has been associated with adverse health effect by a number of studies (Liu et al. 2013; Tao et al. 2012; Wan et al. 2012). Furthermore, during these 5-year period, there were 25 days which were recorded as "severe pollution" (AQI > 300) and out of them, 15 days were found in the year 2013 (Table S1). The highest AQI recorded during these 5 years was 500 on 6 May 2017, where the primary pollutant was PM_{10} with the concentration of 950 $\mu g/m^3$ while the concentration of $PM_{2.5}$ was only 168.6 $\mu g/m^3$. This pollution event is considered as an isolated case as it was caused by a severe dust storm event which originated from the Gobi Desert during 2–7 May 2017 and masked the whole of southeast China, Korean peninsula, and Japan (Zhang et al. 2018).

Table 2 Monthly average concentration of PM$_{2.5}$

| Month | 2013 | | 2014 | | 2015 | | 2016 | | 2017 | |
| | (μg/m^3) | | (μg/m^3) | | (μg/m^3) | | (μg/m^3) | | (μg/m^3) | |
	Range	SD	Range	SD	Range	SD	Range	SD	Range	SD
January	67~371	74	67~287	63	32~255	53	25~194	43	18~186	39
February	29~274	57	26~229	50	22~171	40	25~176	39	25~167	28
March	37~187	35	46~116	18	23~154	26	22~155	37	27~213	37
April	28~142	27	19~139	27	22~104	20	16~79	17	9~77	15
May	20~138	29	25~179	36	24~133	27	15~93	16	13~169	29
June	16~85	20	23~224	43	22~77	13	11~65	14	11~59	11
July	16~53	8	16~81	19	17~72	14	7~41	10	8~65	14
August	20~66	12	21~68	14	11~77	19	9~59	13	9~41	8
September	18~95	18	11~88	24	19~65	12	13~93	21	11~67	13
October	35~275	35	22~180	41	23~116	30	8~86	19	6~102	24
November	41~298	41	24~233	42	17~99	20	9~139	28	32~147	29
December	57~312	57	28~200	32	22~289	65	45~144	26	43~179	36

SD standard deviation

The second highest AQI was 414 on 27 January 2013 where the primary pollutant was PM$_{2.5}$ with the average concentration of 371 μg/m^3 while the concentration of PM$_{10}$ was 342 μg/m^3. Likewise, the lowest concentration of PM$_{2.5}$ on record was 6.3 μg/m^3 on October 12, 2017 when the AQI was 33. Based on the above analysis, it indicates that the air quality in the year 2013 was worse as compared to the other years under study (Table S2) while the year 2017 can be considered as the cleanest year even though it has the highest AQI on record. Corroborated results to this have been reported by Wang et al. (2016). What is promising is that these statistical results suggest that the overall trend of air quality in Wuhan is improving even though the city is still polluted as the daily and annual acceptable limits set in NAAQS are still exceeded. This is thought to be the results of raising awareness of people and several government initiatives such as publishing the daily AQI for major cities and linking the AQI to performance evaluation of local governments (Chen et al. 2012). Note that all these measures aim at combating air pollution problem which is currently a common phenomenon in most of the cities in China.

Pollution process

In the case of this study, a pollution process is defined as a continuous accumulation of air pollutants (PM$_{2.5}$)

which results into increase of AQI value. During these 5-year period, a number of pollution processes have been identified, but for the case of this study, only one pollution process which happened at late November to early December of 2013, will be discussed since most cases look similar. It is worth to mention that out of the 15 days which were identified to have AQI of above 300 (severe pollution) in the year 2013, 8 days were found within these 2 months (November and December). Therefore, describing the pollution process during these months acts as a good representative of what is happening on the ABL during the pollution process. Figure 1 shows clear pollution process from November 28 to December 7, 2013 when the PM$_{2.5}$ concentration increased from 46.2 to 312 μg/m^3 and the AQI raised from 73 (good) to 362 (severe pollution). A closer look on the day before the beginning of the pollution process (November 27) shows that the condition of ABL was better, even though there was small inversion layer (0.5 °C/100 m) with the thickness of 80 m. Above the altitude of 90 m, there was no inversion layer and the wind speed at the ABL was very high, reaching 15 m/s (Fig. 2 (a)). This high wind speed which is observed throughout the ABL is a favorable condition for horizontal mixing of pollutants with clean air (Quan et al. 2013), as a result, the day recorded the PM$_{2.5}$ concentration of 64.6 μg/m^3 and the AQI of 87, indicating that the air quality was "good" (Table 1).

Fig. 1 Daily average PM$_{2.5}$ and AQI for Wuhan from November to December 2013 where the red line shows the daily average acceptable limit
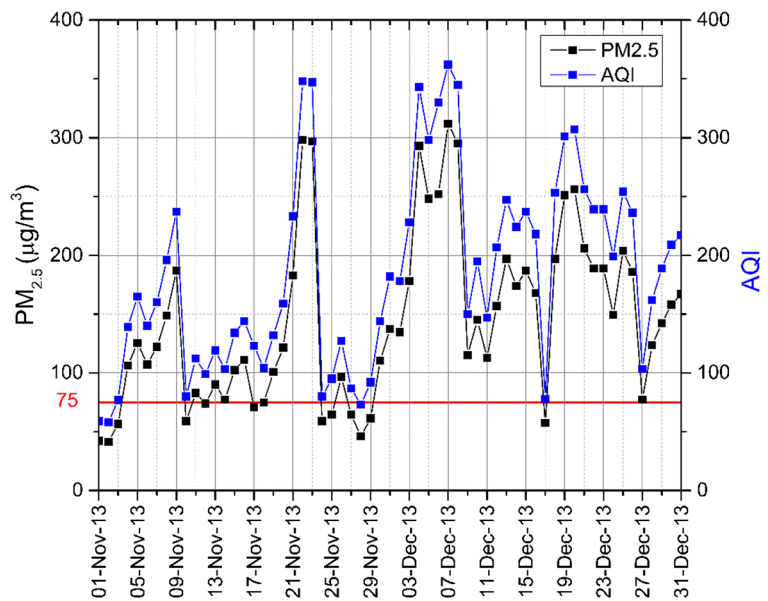
A different scenario on the condition of the ABL began to be observed on November 28 (Fig. 2 (b)) as the strength of inversion layer was strengthened and the speed of wind was weakened significantly (Table 3). During this day, the strength of inversion layer increased to 3 °C/100 m and the wind speed decreased to 1 m/s. These observed conditions at the ABL are not favorable for pollutant dispersion as they limit horizontal and vertical mixing of air pollutants. Comparable results to this have been reported by Yassin et al. (2018) in Kuwait that whenever the mixing layer height decreases, the concentrations of air pollutants were observed to increase. Figure 2 (c and d) shows the condition of the ABL continued to worsen, where the strength of the inversion layer continued to build up (3.3~5 °C/100 m), and the thickness also continued to grow bigger (110~240 m). On 1 December, the condition of ABL was far worse than the previous days, as the wind was calm and the thickness of the inversion layer continued to increase (Fig. 2 (e)). This condition is thought to favor more accumulation of pollutants as horizontal and vertical mixing capacity of ABL was further weakened; therefore, pollutants were not distributed to other areas and got mixed with clean air. During this day, there was an increase of concentration of PM$_{2.5}$ by 197% as compared to 3 previous days and the AQI of this day was 182, indicating the condition of the air is "moderately polluted." There was slight decrease in the concentration of PM$_{2.5}$ (2.8 μg/m³) and AQI on 2 December because on this day, the wind speed which reached

12 m/s was recorded at the altitude of 790 m (Fig. 2 (f)). Note that, on the previous day, the wind speed at ground was calm and at about 790 m, the wind speed was only 4 m/s. Even though the humidity on December 3 was the highest (99%), the concentration of PM$_{2.5}$ and AQI increased to 178 μg/m³ and 228 (heavy pollution), respectively, as a result of calm wind and increased strength of inversion layer (Fig. 2 (g)).

Severe pollution (AQI = 343) and PM$_{2.5}$ concentration of 293 μg/m³ were recorded on December 4, as a result of pollutant accumulation from the previous days. On this day, the wind speed at the inversion layer which already limited vertical mixing was small, ranging between 1 and 4 m/s, the speed which is not higher enough to favor horizontal movement of air pollutant. Therefore, the condition on this day was not favorable for both vertical and horizontal mixing of air pollutants, as a result, more pollutants were allowed to accumulate (Fig. 2 (h)). The following 2 days (December 5 and 6) observed a decrease in PM$_{2.5}$ concentration and AQI moderately due to increase in relative humidity near the ground (Fig. 2 (i)) and increase in wind speed which reached about 12 m/s at the altitude of 760 m (Fig. 2 (j)). December 7 was the peak of this pollution process as the recorded PM$_{2.5}$ concentration was 312 μg/m³ and the AQI was 362 which indicate "severe pollution." As compared to the previous day (December 6), the condition of ABL on this day (December 7) was further worsened (Fig. 2 (k)). For instance, on this day (previous day), ground wind speed was 1 m/s (2 m/s) and reached 2 m/s (12 m/s) at the altitude of
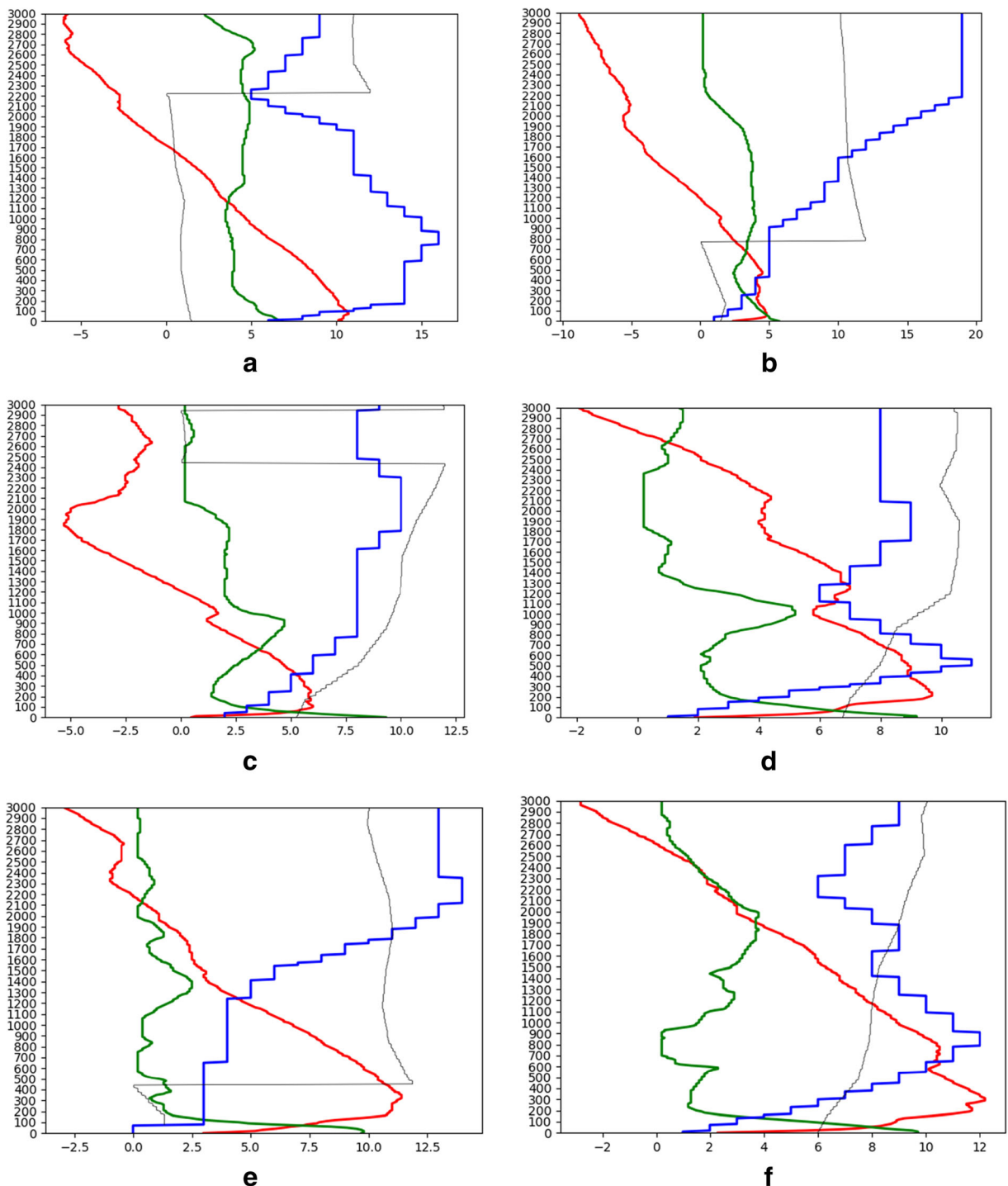
Fig. 2 Vertical structure of the atmosphere on 27 November 2013, $PM_{2.5} = 36.6$ μg/m3 and AQI = 52 (**a**); 28 November 2013, $PM_{2.5} = 88.6$ μg/m3 and AQI = 117 (**b**); 29 January 2013, $PM_{2.5} = 119.2$ μg/m3 and AQI = 156 (**c**); 30 November 2013, $PM_{2.5} = 173$ μg/m3 and AQI = 223 (**d**); 1 December 2013, $PM_{2.5} = 201$ and AQI = 251 (**e**); 2 December 2013, $PM_{2.5} = 239$ and AQI = 289 (**f**); 3 December 2013, $PM_{2.5} = 205$ and AQI = 255 (**g**); 4 December 2013, $PM_{2.5} = 309$ and AQI = 359 (**h**); 5 December 2013, $PM_{2.5} = 275$ and AQI = 326 (**i**); 6 December 2013, $PM_{2.5} = 310$ and AQI = 360 (**j**); 7 December 2013, $PM_{2.5} = 310$ and AQI = 360 (**k**); 9 December 2013, $PM_{2.5} = 310$ and AQI = 360 (**l**) showing the profile of temperature (red line, °C), relative humidity (green line, %), wind velocity (blue line, m/s), and dominant wind direction (gray line) during the pollution process. The number on X-axis is the result after dividing the relative humidity value by 10 and the wind direction angle by 30, while temperature and wind speed remain the same
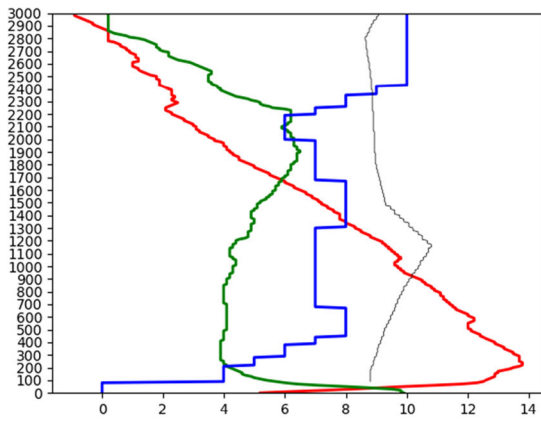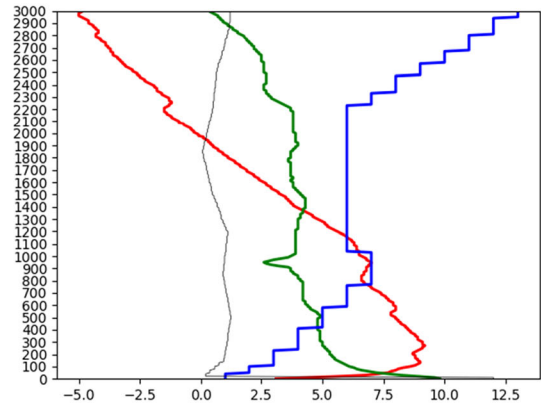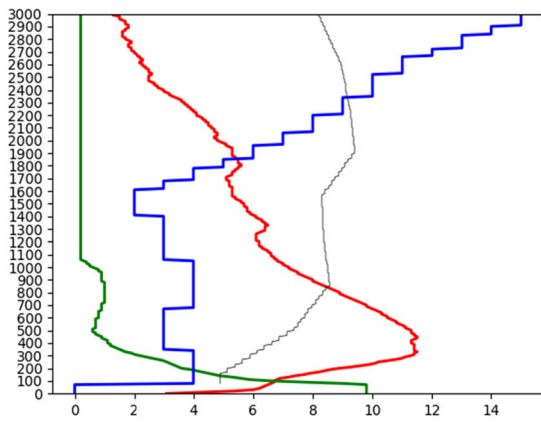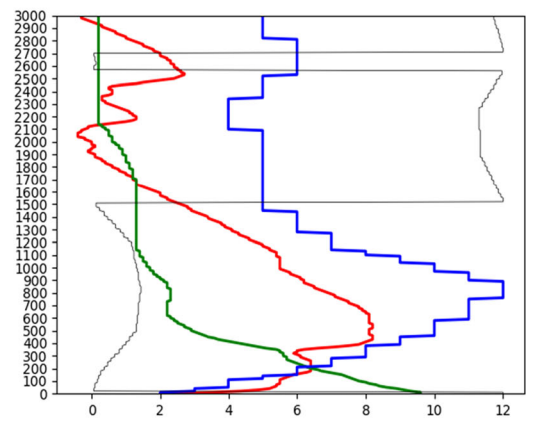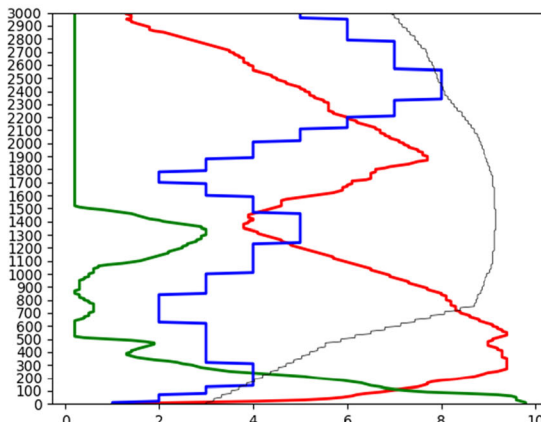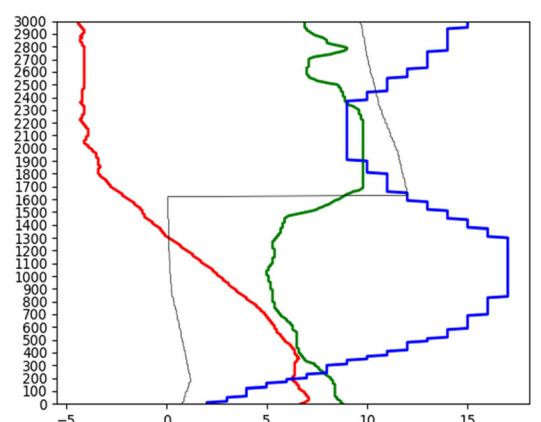
Fig. 2 continued.

Table 3 Ground meteorological variables during PM$_{2.5}$ pollution process

Date	Air temperature (°C)	Humidity (%)	Wind speed (m/s)	Wind direction	Pressure (hPa)	Characteristics of inversion layer		
						Strength (°C/100 m)	Altitude (m)	Thickness (m)
27 November 13	10.3	68	6	45	1022	0.5	10	80
28 November 13	2.4	57	1	45	1029	3	0	80
29 November 13	0.5	93	2	158	1026	5	0	110
30 November 13	1.9	88	1	203	1022	3.3	0	240
01 December 13	3.0	97	0	C	1023	2.4	0	350
02 December 13	2.3	97	1	180	1018	3.2	0	310
03 December 13	5.2	99	0	C	1017	3.6	0	240
04 December 13	3.1	98	1	360	1022	2	0	300
05 December 13	3.1	98	0	C	1018	2.5	0	330
06 December 13	2.3	95	2	360	1024	1.3	0	460
07 December 13	1.1	98	1	90	1018	2.4	0	350
09 December 13	6.7	88	2	23	1022	0.4	0	*50*
Average	3.5	90	1.4	360*	1022	2	0	277

*Dominant wind direction

760 m, strength of inversion was 2.4 °C/100 m (1.3 °C/100 m), and the thickness of the inversion layer was 350 m (460 m) (Table 3). These general conditions of ABL are not favorable for pollutant dispersion as they have further weakened the horizontal and vertical mixing capacity of the ABL, as a result, more pollutants accumulate in Wuhan atmosphere. Corroborated results to this have been reported by Lee et al. (2013) as they found that the thickness of inversion layer was high during the polluted days as compared to periods before and after the polluted days. This is because an inversion layer has the tendency of trapping pollutants within the inversion layer, as a result, it limits the exchange of pollutants and clean air at free troposphere (Quan et al. 2013). Nevertheless, 2 days later (December 9), the air condition improved significantly; the concentration of PM$_{2.5}$ and AQI dropped to 115 μg/m^3 and 150 ("slightly polluted"), respectively as a result of improved ABL condition. On this day, the ground inversion layer which was observed only in the first 50 m was significantly weakened to 0.4 °C/100 m. Furthermore, the ABL was more humid than the previous day and the wind speed was high, reaching 16 m/s at the altitude of 850 m (Fig. 2 (l)). These observed conditions during this period are favorable for vertical and horizontal distribution of pollutants (Mbululo et al. 2017).

Analysis of the cluster mean back trajectory result for November and December 2013 identifies four major air masses, two among them contributed significant amount of air pollutants. The first important air mass is associated with local pollution which accounted for 58.06% of the total loading, while the second air mass which accounted for 29.03% and the third (8.39%), originated in Inner Mongolia and passed through Shaanxi, Shanxi, and Henan provinces before they arrived in Wuhan. The fourth air mass which accounted for 4.52% originated in southern Russia and passed through Inner Mongolia before it entered the most serious polluted area of Hebei and Henan province (Fig. 3 (a)). Since back trajectory results cannot stimulate the values of daily PM$_{2.5}$ level caused by PSA (Jeong et al. 2011; Xin et al. 2016), further analysis was done by using PSCF. Figure 3 (b) shows the results of PSCF analysis, where red color represents high contribution level of PSA while blue color represents low contribution of PM$_{2.5}$ concentration. As it can be seen on the map, the higher WPSCF value of above 1 was mainly from Wuhan, which indicates that the pollutants were mainly of local origin and WPSCF value of above 0.8 was mainly from Hunan and Henan provinces. These results compliment the results which have been reported on the ABL that during the pollution process, the vertical and horizontal mixing capacity was weak, which resulted into pollutant accumulation. It therefore suggests that the local air masses played a significant role in this observed pollution process.
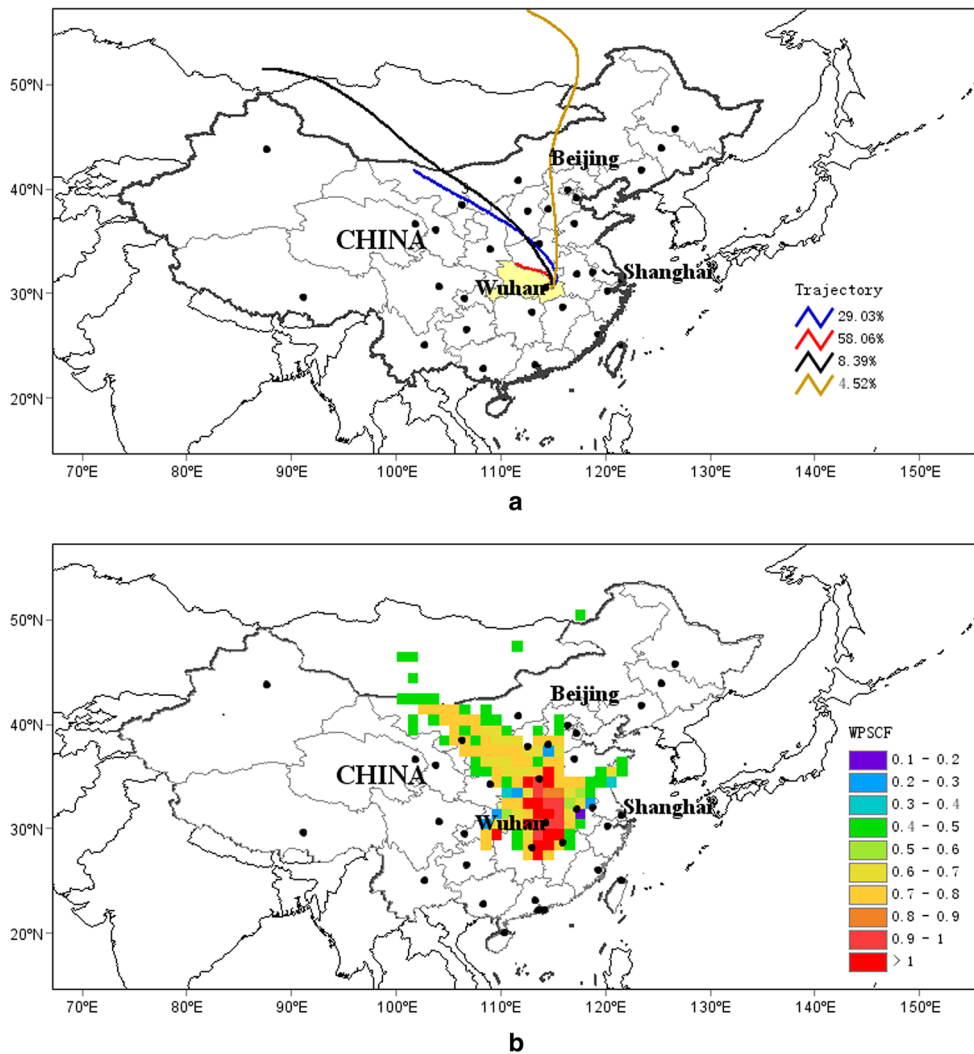
Fig. 3 Maps showing cluster mean back trajectories for November and December (**a**) and spatial distribution of WPSCF (**b**)

Conclusion

Analysis of six air pollutants from 2013 to 2017 shows that PM_{10}, $PM_{2.5}$, NO_2, and O_3 exceeded the daily and annual acceptable limits set in NAAQS at different levels except SO_2 and CO. During these 5 years, 2013, 2014, 2014, 2016, and 2017, $PM_{2.5}$ was higher than the daily average acceptable limits for 175, 160, 121, 91, and 71 days, respectively. These results indicate that about a half of the years 2013 and 2014 and one third (4 months) of 2014 were polluted by $PM_{2.5}$. Moreover, the annual average concentration of $PM_{2.5}$ of the year 2013, 2014, 2015, 2016, and 2017 were 94.4 μg/m^3, 80.4 μg/m^3, 69.4 μg/m^3, 57.5 μg/m^3, and 53.2 μg/m^3, respectively, the

concentrations of which are higher than the annual acceptable limit of 35 μg/m^3. The days which exceeded the daily average acceptable limit of PM_{10}, NO_2, and O_3 during these 5 years were in the range of 30~111, 19~80, and 36~143 days, respectively. Based on the number of days which comply with NAAQS, the year 2017 is regarded as the cleanest year while the year 2013 is regarded as the most polluted year. During the pollution process, the condition of ABL was dominated by strong ground inversion layer and weak winds, the condition which weakens the horizontal and vertical transport mixing of air pollutants. As a result, pollutants were accumulated and restrained from mixing with clean air. Likewise, the cluster analysis of air mass back trajectory shows that the pollutants were

mainly of local origins since higher value of WPSCF was mainly dominant in Wuhan. This therefore suggests that trans-boundary movement of air pollutants was not an important factor during this pollution process.

Publisher's Note   Springer Nature remains neutral with regard to jurisdictional claims in published maps and institutional affiliations.

References

Acciai, C., Zhang, Z., Wang, F., Zhong, Z., & Lonati, G. (2017). Characteristics and source analysis of trace elements in PM2.5 in the urban atmosphere of Wuhan in spring. *Aerosol and Air Quality Research, 17*, 2224–2234. https://doi.org/10.4209/aaqr.2017.06.0207.

Chen, Y., Jin, G. Z., Kumar, N., & Shi, G. (2012). Gaming in air pollution data? Lessons from China. *Journal of Economic Analysis & Policy, Advances, 13*(3), 1–42. https://doi.org/10.3386/w18729.

Dimitriou, K. (2015). The dependence of PM size distribution from meteorology and local-regional contributions, in Valencia (Spain) – a CWT model approach. *Aerosol and Air Quality Research, 15*, 1979–1989. https://doi.org/10.4209/aaqr.2015.03.0162.

Dimitriou, K., & Kassomenos, P. (2014). Indicators reflecting local and transboundary sources of PM2.5 and PMCOARSE in Rome - impacts in air quality. *Atmospheric Environment, 96*, 154–162. https://doi.org/10.1016/j.atmosenv.2014.07.029.

Feng, Z., Hu, E., Wang, X., Jiang, L., & Liu, X. (2015). Ground-level O₃ pollution and its impacts on food crops in China: a review. *Environmental Pollution, 199*, 42–48. https://doi.org/10.1016/j.envpol.2015.01.016.

GB3095 (2012). People's Republic of China National Ambient Air Quality Standard. China. Available online: http://210.72.1.216:8080/gzaqi/Document/gjzlbz.pdf. Accessed 07 Dec 2017.

HJ633 (2012). Technical requirements for ambient air quality index (AQI) (Trial Implementation), People's Republic of China, National Environmental Protection Standard. China. Available online: http://210.72.1.216:8080/gzaqi/Document/aqijsgd.pdf Accessed 07 Dec 2017.

Hu, X. M., Ma, Z., Lin, W., Zhang, H., Hu, J., Wang, Y., Xu, X., Fuentes, J. D., & Xue, M. (2014). Impact of the Loess Plateau on the atmospheric boundary layer structure and air quality in

the North China Plain: a case study. *Science of the Total Environment, 499*, 228–237. https://doi.org/10.1016/j.scitotenv.2014.08.053.

Inomata, Y., Igarashi, Y., Chiba, M., Shinoda, Y., & Takahashi, H. (2009). Dry and wet deposition of water-insoluble dust and water-soluble chemical species during spring 2007 in Tsukuba, Japan. *Atmospheric Environment, 43*(29), 4503–4512. https://doi.org/10.1016/j.atmosenv.2009.06.048.

Jeong, U., Kim, J., Lee, H., Jung, J., Kim, Y. J., Song, C. H., & Koo, J. H. (2011). Estimation of the contributions of long range transported aerosol in East Asia to carbonaceous aerosol and PM concentrations in Seoul, Korea using highly time resolved measurements: a PSCF model approach. *Journal of Environmental Monitoring, 13*(7), 1905–1918. https://doi.org/10.1039/c0em00659a.

Lee, S., Ho, C. H., Lee, Y. G., Choi, H. J., & Song, C. K. (2013). Influence of transboundary air pollutants from China on the high-PM10 episode in Seoul, Korea for the period October 16–20, 2008. *Atmospheric Environment, 77*, 430–439. https://doi.org/10.1016/j.atmosenv.2013.05.006.

Li, G., Bei, N., Cao, J., Wu, J., Long, X., Feng, T., et al. (2017). Widespread and persistent ozone pollution in eastern China during the non-winter season of 2015: observations and source attributions. *Atmospheric Chemistry and Physics, 17*, 2759–2774. https://doi.org/10.5194/acp-17-2759-2017.

Li, X., Wang, Y., Zhao, H., Hong, Y., Liu, N., & Ma, Y. (2018). Characteristics of pollutants and boundary layer structure during two haze events in summer and autumn 2014 in Shenyang, Northeast China. *Aerosol and Air Quality Research, 18*, 386–396. https://doi.org/10.4209/aaqr.2017.03.0100.

Liu, T., Tian, T., Hui, Y., Jun, Y., Qian, X., Yan, H., et al. (2013). The short-term effect of ambient ozone on mortality is modified by temperature in Guangzhou, China. *Atmospheric Environment, 76*, 59–67. https://doi.org/10.1016/j.atmosenv.2012.07.011.

Lu, H.-Y., Mwangi, J. K., Wang, L.-C., Wu, Y.-L., Tseng, C.-Y., & Chang, K.-H. (2016). Atmospheric PM2.5 characteristics and long-term trends in Tainan city, Southern Taiwan. *Aerosol and Air Quality Research, 16*(10), 2488–2511. https://doi.org/10.4209/aaqr.2016.07.0332.

Lyu, X. P., Chen, N., Guo, H., Zeng, L., Zhang, W., Shen, F., et al. (2016). Chemical characteristics and causes of airborne particulate pollution in warm seasons in Wuhan, central China. *Atmospheric Chemistry and Physics, 16*(16), 10671–10687. https://doi.org/10.5194/acp-16-10671-2016.

Mbululo, Y., Qin, J., & Yuan, Z. (2017). Evolution of atmospheric boundary layer structure and its relationship with air quality in Wuhan, China. *Arabian Journal of Geosciences, 10*(22), 1–12. https://doi.org/10.1007/s12517-017-3257-9.

Polissar, A. V., Hopke, P. K., Paatero, P., Kaufmann, Y. J., Hall, D. K., Bodhaine, B. A., et al. (1999). The aerosol at Barrow, Alaska: long-term trends and source locations. *Atmospheric Environment, 33*, 2441–2458.

Quan, J., Gao, Y., Zhang, Q., Tie, X., Cao, J., Han, S., Meng, J., Chen, P., & Zhao, D. (2013). Evolution of planetary boundary layer under different weather conditions, and its impact on aerosol concentrations. *Particuology, 11*(1), 34–40. https://doi.org/10.1016/j.partic.2012.04.005.

Ran, L., Zhao, C., Geng, F., Tie, X., Tang, X., Peng, L., Zhou, G., Yu, Q., Xu, J., & Guenther, A. (2009). Ozone photochemical

production in urban Shanghai, China: analysis based on ground level observations. *Journal of Geophysical Research, 114*, 1–14. https://doi.org/10.1029/2008JD010752.

Rolph, G., Stein, A., & Stunder, B. (2017). Real-time environmental applications and display system: READY. *Environmental Modelling and Software, 95*, 210–228. https://doi.org/10.1016/j.envsoft.2017.06.025.

Stein, A. F., Draxler, R. R., Rolph, G. D., Stunder, B. J. B., Cohen, M. D., & Ngan, F. (2015). NOAA's HYSPLIT atmospheric transport and dispersion modeling system. *Bulletin of the American Meteorological Society, 96*(12), 2059–2077. https://doi.org/10.1175/BAMS-D-14-00110.1.

Tang, G., Zhu, X., Xin, J., Hu, B., Song, T., Sun, Y., Zhang, J., Wang, L., Cheng, M., Chao, N., Kong, L., Li, X., & Wang, Y. (2017). Modelling study of boundary-layer ozone over northern China—part I: ozone budget in summer. *Atmospheric Research, 187*, 128–137. https://doi.org/10.1016/j.atmosres.2016.10.017.

Tao, Y., Huang, W., Huang, X., Zhong, L., Lu, S., Li, Y., et al. (2012). Estimated acute effects of ambient ozone and nitrogen dioxide on mortality in the Pearl River Delta of Southern China. *Environmental Health Perspectives, 120*(3), 393–398.

Wan, W., Xie, X., & Zhang, S. (2012). Health effect valuation of ground-level ozone control in Beijing and its surrounding areas, China. *Advanced Materials Research, 360*, 585–589. https://doi.org/10.4028/www.scientific.net/AMR.356-360.585.

Wang, Y. Q., Zhang, X. Y., & Draxler, R. R. (2009). TrajStat: GIS-based software that uses various trajectory statistical analysis methods to identify potential sources from long-term air pollution measurement data. *Environmental Modelling and Software, 24*(8), 938–939. https://doi.org/10.1016/j.envsoft.2009.01.004.

Wang, S., Yu, S., Yan, R., Zhang, Q., Li, P., Wang, L., Liu, W., & Zheng, X. (2016). Characteristics and origins of air pollutants in Wuhan, China, based on observations and hybrid receptor models. *Journal of the Air & Waste Management Association, 2247*, 10962247.2016.1240724–10962247.2016.1240753. https://doi.org/10.1080/10962247.2016.1240724.

Wang, T., Xue, L., Brimblecombe, P., Fat, Y., Li, L., & Zhang, L. (2017). Ozone pollution in China: a review of concentrations, meteorological influences, chemical precursors, and effects. *Science of the Total Environment, 575*, 1582–1596. https://doi.org/10.1016/j.scitotenv.2016.10.081.

WHO. (2016). Ambient air pollution: a global assessment of exposure and burden of diseases. Geneva, Switzerland. http://apps.who.int/iris/bitstream/10665/250141/1/9789241511353-eng.pdf?ua=1. Accessed 06 Nov 2017.

Wu, M., Wu, D., Fan, Q., Wang, B. M., Li, H. W., & Fan, S. J. (2013). Observational studies of the meteorological characteristics associated with poor air quality over the Pearl River Delta in China. *Atmospheric Chemistry and Physics, 13*, 10755–10766. https://doi.org/10.5194/acp-13-10755-2013.

Xin, Y., Wang, G., & Chen, L. (2016). Identification of long-range transport pathways and potential sources of PM10 in Tibetan Plateau uplift area: case study of Xining, China in 2014. *Aerosol and Air Quality Research, 16*, 1044–1054. https://doi.org/10.4209/aaqr.2015.05.0296.

Xu, G., Jiao, L., Zhang, B., Zhao, S., Yuan, M., Gu, Y., & Liu, J. (2017). Spatial and temporal variability of the PM2.5/PM10 ratio in Wuhan, Central China. *Aerosol and Air Quality Research, 17*(2016), 741–751. https://doi.org/10.4209/aaqr.2016.09.0406.

Yassin, M. F., Al-Shatti, L. A., & Al Rashidi, M. S. (2018). Assessment of the atmospheric mixing layer height and its effects on pollutant dispersion. *Environmental Monitoring and Assessment, 190*(7). https://doi.org/10.1007/s10661-018-6737-9.

Zeng, Y., & Hopke, P. K. (1989). A study of the sources and acid precipitation in Ontario, Canada. *Atmospheric Environment, 23*(7), 1499–1509.

Zhang, X. X., Sharratt, B., Liu, L. Y., Wang, Z. F., Pan, X., Le, Lei., et al. (2018). East Asian dust storm in May 2017: Observations, modelling, and its influence on the Asia-Pacific region. *Atmospheric Chemistry and Physics, 18*(11), 8353–8371. https://doi.org/10.5194/acp-18-8353-2018.